

Fei-Chi Yang, Yuchen Zhang and Maikel C. Rheinstädter

Department of Physics and Astronomy, McMaster University, Hamilton, Ontario, Canada

**ABSTRACT**

Hair is a filamentous biomaterial consisting mainly of proteins in particular keratin. The structure of human hair is well known: the *medulla* is a loosely packed, disordered region near the centre of the hair surrounded by the *cortex*, which contains the major part of the fibre mass, mainly consisting of keratin proteins and structural lipids. The *cortex* is surrounded by the *cuticle*, a layer of dead, overlapping cells forming a protective layer around the hair. The corresponding structures have been studied extensively using a variety of different techniques, such as light, electron and atomic force microscopes, and also X-ray diffraction. We were interested in the question how much the molecular hair structure differs from person to person, between male and female hair, hair of different appearances such as colour and waviness. We included hair from parent and child, identical and fraternal twins in the study to see if genetically similar hair would show similar structural features.

The molecular structure of the hair samples was studied using high-resolution X-ray diffraction, which covers length scales from molecules up to the organization of secondary structures. Signals due to the coiled-coil phase of  $\alpha$ -helical keratin proteins, intermediate keratin filaments in the *cortex* and from the lipid layers in the cell membrane complex were observed in the specimen of all individuals, with very small deviations. Despite the relatively small number of individuals (12) included in this study, some conclusions can be drawn. While the general features were observed in all individuals and the corresponding molecular structures were almost identical, additional signals were observed in some specimen and assigned to different types of lipids in the cell membrane complex. Genetics seem to play a role in this composition as identical patterns were observed in hair from father and daughter and identical twins, however, not for fraternal twins. Identification and characterization of these features is an important step towards the detection of abnormalities in the molecular structure of hair as a potential diagnostic tool for certain diseases.

Submitted 7 August 2014  
Accepted 22 September 2014  
Published 14 October 2014

Corresponding author  
Maikel C. Rheinstädter,  
rheinstadter@mcmaster.ca

Academic editor  
Mikko Karttunen

Additional Information and  
Declarations can be found on  
page 15

DOI 10.7717/peerj.619

© Copyright  
2014 Yang et al.

Distributed under  
Creative Commons CC-BY 4.0

**Subjects** Biophysics

**Keywords** Human hair, Molecular structure, X-ray diffraction, Keratin, Intermediate filament, Coiled-coil proteins, Alpha helix, Cell membrane complex

**INTRODUCTION**

Human scalp hair is a bio-synthesized material that has a complex internal structure. The adult human hair is around 20–180  $\mu\text{m}$  in width, and generally grows to a length of approximately 90 cm. It consists of many layers including the *cuticle*, the *cortex* and the *medulla*. These layers are bound together by the cell membrane complex (Robbins, 2012).

**OPEN ACCESS**

The structure of human hair is well known and in particular X-ray diffraction revealed details of molecular structure and organization within hair (Fraser *et al.*, 1986; Briki *et al.*, 2000; Busson, Engstrom & Doucet, 1999; Randebrook, 1964; Fraser, MacRae & Rogers, 1962; Kreplak *et al.*, 2001b; Wilk, James & Amemiya, 1995; Pauling & Corey, 1951; Ohta *et al.*, 2005; Astbury & Street, 1932; Astbury & Woods, 1934; Astbury & Sisson, 1935; Franbourg *et al.*, 2003; Rafik, Doucet & Briki, 2004; James *et al.*, 1999; Veronica & Amemiya, 1998; Briki *et al.*, 1999; James, 2001). In particular microbeam small angle X-ray scattering techniques enables the determination of hair structure with a high spatial resolution (Iida & Noma, 1993; Busson, Engstrom & Doucet, 1999; Kreplak *et al.*, 2001b; Ohta *et al.*, 2005; Kajiura *et al.*, 2006). It is a long-standing question whether changes in the molecular structure of nail or hair can be related to certain diseases and potentially be used as a diagnostic tool. Such a technique would in particular be interesting and relevant as simple, non-invasive screening method for cancer (James *et al.*, 1999; Briki *et al.*, 1999; James, 2001). Abnormal kinky hair is, for instance, characteristic of giant axonal neuropathy (Berg, Rosenberg & Asbury, 1972).

The purpose of this study is to use X-ray diffraction to analyze the structure of human scalp hair for individuals with differing characteristics. The 12 individuals in this study include hair from men and women and hair of different colour and appearance, such as straight, wavy and curly. In addition to appearance, the study also includes hair from a father and daughter, a pair of identical and a pair of fraternal twins to include genetic similarities. All hair was collected from healthy individuals and care was taken that the hair was not permed or dyed before the experiments.

Signals due to the coiled-coil organization of  $\alpha$ -helical keratin proteins and intermediate filaments in the *cortex*, and lipids in the cell membrane complex were observed in the hair of all individuals. While these general features occur independent of gender or appearance of the hair with a very small standard deviation in the underlying molecular dimensions, we find significant differences between individuals in the composition of the plasma membrane in the cell membrane complex. Genetics appear to be the most important factor that determines membrane composition, as no or little differences were observed in genetically related hair samples, rather than external factors such as nutrition or hair care products.

### Properties of human hair

The *cuticle* is the outermost layer formed by flat overlapping cells in a scale-like formation (Robbins, 2012). These cells are approximately 0.5  $\mu\text{m}$  thick, 45–60  $\mu\text{m}$  long and found at 6–7  $\mu\text{m}$  intervals (Robbins, 2012). The outermost layer of the *cuticle*, the epicuticle, is a lipo-protein membrane that is estimated to be 10–14 nm thick (Swift & Smith, 2001). Beneath that is the A layer with a high cysteine content and a thickness of 50–100 nm, the exocuticle with again a high cysteine content and a highly variable thickness ranging from 50 to 300 nm, and the endocuticle with a low cysteine content and a thickness also ranging from 50 to 300 nm.

The majority of hair fibre is the cortex which contains spindle shaped cells that lie parallel along the fibre axis. These cortical cells were found to be approximately 1–6  $\mu\text{m}$

in diameter and 50–100  $\mu\text{m}$  in length (Randebrook, 1964). In wool fibres as well as human hair, the cortical cells were observed to be divided into different regions termed ortho-cortex, paracortex and mesocortex (Mercer, 1953). The difference in distribution of these cell types is an important factor for determining the curvature of the hair fibre (Kajiura et al., 2006). In particular, straight hair tends to have symmetrical distribution of the ortho- and paracortices whereas curly hair tends to have a non-symmetrical distribution of these cortical cells (Kajiura et al., 2006). Most of the cortical cells are composed of a protein known as keratin (Robbins, 2012).

At the molecular level, keratin is a helical protein (Pauling & Corey, 1950). There are two types of keratin fibres that exist in hair: type I with acidic amino acid residues and type II with basic amino residues. One strand of type I fibre and one strand of type II fibre spiral together to form coiled-coil dimers. In turn, these dimers coil together in an antiparallel manner to form tetramers (Crewther et al., 1983; Fraser et al., 1988).

When tetramers are connected from head to tail, they are known as protofilaments (Robbins, 2012). These tetramers or protofilaments are believed to interact together to form a single intermediate filament which is approximately 75–90  $\text{\AA}$  in diameter. The current model of an intermediate filament was proposed in the 1980's and it involves 7 protofilaments surrounding a single core protofilament (Robbins, 2012; Fraser et al., 1988). The intermediate filaments then aggregate together to form macro-filaments with a diameter of 1000 to 4000  $\text{\AA}$  (Robbins, 2012; Randebrook, 1964). Between the intermediate filaments is a matrix consisting of keratin associated proteins, which are irregular in structure. The macro-fibrils consisting of intermediate filaments and the surrounding matrix are the basic units of the cortical cell.

The cell membrane complex is the material that glues hair cells together. There exist various types of cell membrane complexes: *cuticle–cuticle*, *cuticle–cortex* and *cortex–cortex* depending on the location (Robbins, 2012). The general membrane structure is one 15 nm proteinous delta layer sandwiched by two 5 nm lipid beta layers (Rogers, 1959). Much speculation still exist regarding the precise structure of the beta and delta layers. However, it has been determined that 18-methyl eicosanoic acid, a covalently bound fatty acid, exists in the upper beta layer in the *cuticle–cuticle* but not in *cortex–cortex* membranes (Ward & Lundgren, 1954). In fact, most of the fatty acids in beta layers of membranes in the *cuticle–cuticle* are covalently bound and most of the fatty acids in the beta layers of *cortex–cortex* are non-covalently bound (Robbins, 2012). Further evidence suggests that the fatty acids in *cuticle–cuticle* membranes are organized in a monolayer whereas the fatty acids in *cortex–cortex* cell membranes are bilayers (Robbins, 2012). The *cuticle–cortex* cell membrane complex is then a mixture of the two, with the side facing the *cuticle* similar to *cuticle–cuticle* membranes and the side facing the *cortex* similar to *cortex–cortex* membranes (Robbins, 2012).

**Table 1** List of all hair samples in this study. The individuals include men and women and hair of different appearance, such as thickness, colour and waviness, and also genetically related hair samples from a father and daughter, a pair of identical and a pair of fraternal twins. Labeling agrees with the data shown in Fig. 1.

Subject	Gender	Diameter( $\mu\text{m}$ ) $\pm$ SD	Colour	Appearance	Special comment
1	F	30 $\pm$ 3	light blonde	straight	daughter
2	M	49 $\pm$ 5	brown/grey	curly	father
3	F	74 $\pm$ 7	black	wavy	–
4	M	50 $\pm$ 5	light brown	curly	–
5	F	49 $\pm$ 5	blonde	curly	–
6	F	43 $\pm$ 4	light brown	straight	–
7	F	61 $\pm$ 6	light brown	wavy	–
8	F	49 $\pm$ 5	black	wavy	–
9	F	31 $\pm$ 3	blonde	wavy	identical twin
10	F	66 $\pm$ 7	black	straight	fraternal twin
11	F	69 $\pm$ 7	black	straight	fraternal twin
12	F	48 $\pm$ 5	blonde	curled	identical twin

## MATERIALS AND METHODS

### Preparation of hair samples

This research was approved by the Hamilton Integrated Research Ethics Board (HIREB) under approval number 14-474-T. Written consent was obtained from all participating individuals. Scalp hair samples were gathered from 12 adults of various age, gender, ethnicities, hair colour and hair curvature. It is of interest to note that there are 3 pairs of study participants with genetic relations including a father and daughter, fraternal twins and identical twins. Characteristics of the samples are listed in Table 1.

The hair samples gathered were cut into strands around 3 cm long. Care was taken to not stretch or deform the hair strands during this process. For each subject, around 10 strands were taped onto a flexible cardboard apparatus as shown in Fig. 2. The cut-out at the middle of the apparatus is where scattering occurs on the hair sample. The cardboard apparatus is then mounted vertically onto the loading plate of the Biological Large Angle Diffraction Experiment (BLADE) using sticky putty as shown in Fig. 2. All hair samples were measured at room temperature and humidity of 22 °C and 50% RH.

### X-ray diffraction experiment

X-ray diffraction data was obtained using the Biological Large Angle Diffraction Experiment (BLADE) in the Laboratory for Membrane and Protein Dynamics at McMaster University. BLADE uses a 9 kW (45 kV, 200 mA) CuK $\alpha$  Rigaku Smartlab rotating anode at a wavelength of 1.5418 Å. Focusing multi-layer optics provided a high intensity parallel beam with monochromatic X-ray intensities up to 10<sup>10</sup> counts/(s  $\times$  mm<sup>2</sup>) at the sample position. In order to maximize the scattered intensity, the hair strands were aligned parallel to the parallel beam for maximum illumination. The slits were set such that about 15 mm of the hair strands were illuminated with a width of about 100  $\mu\text{m}$ . The effect of this

particular beam geometry is seen in the 2-dimensional data in Fig. 1: while it produces a high resolution along the equator, the main beam is significantly smeared out in the  $q_z$ -direction up to  $q_z$ -values of about  $0.5 \text{ \AA}^{-1}$ , limiting the maximum observable length scale to about  $13 \text{ \AA}$ .

The diffracted intensity was collected using a point detector. Slits and collimators were installed between X-ray optics and sample, and between sample and detector, respectively. By aligning the hair strands in the X-ray diffractometer, the molecular structure along the fibre direction and perpendicular to the fibres could be determined. We refer to these components of the total scattering vector,  $\vec{Q}$ , as  $q_z$  and  $q_{\parallel}$ , respectively, in the following. An illustration of  $q_z$  and  $q_{\parallel}$  orientations is shown in Fig. 3. The result of an X-ray experiment is a 2-dimensional intensity map of a large area of the reciprocal space of  $-2.5 \text{ \AA}^{-1} < q_z < 2.5 \text{ \AA}^{-1}$  and  $-2.5 \text{ \AA}^{-1} < q_{\parallel} < 2.5 \text{ \AA}^{-1}$ . The corresponding real-space length scales are determined by  $d = 2\pi/|Q|$  and cover length scales from about  $3$  to  $90 \text{ \AA}$ , incorporating typical molecular dimensions and distances for secondary protein and lipid structures.

Integration of the 2-dimensional data was performed using Matlab, MathWorks. By adding up the peak intensities along the  $q_z$  and the  $q_{\parallel}$  directions, 1-dimensional data along each of the two directions were produced. The  $q_z$  intensity was integrated azimuthally for an angle of 25 degrees over the meridian. The  $q_{\parallel}$  intensity was integrated azimuthally for an angle of 25 degrees over the equator, as depicted in Fig. 3.

The fitting process is performed on both the 1-dimensional  $q_z$  and the  $q_{\parallel}$  data produced from integration. Distinguishable peaks were observed and fitted with the least numbers of Lorentzian peak functions with an exponential decay background of the form  $(a \cdot q^b + c)$  in the first run. Initial Parameters were chosen based on the observed positions, widths and heights of the peaks and free to move through the entire  $q$ -range. The criterion for the final parameters was to minimize the mean square of the difference between data intensity and the fitted intensity. If the fitted intensity cannot conform to the shape of the data intensity, more peaks will be added in the following runs until a good fit is acquired. This process was repeated for all 12 subjects and performed with little or no consultation of previous fittings to minimize bias.

As for the SAXS data, Gaussian functions are used instead. We note that the use of optical components in the beam path has an impact on the shape of the observed Bragg peaks: instead of Lorentzian or Bessel peak functions, Gaussian peak profiles were found to best describe the SAXS peaks. The fitting process was the same as mentioned before: three Gaussians were fitted to the SAXS data using free-to-move parameters and an exponential decay background. However, for some subjects, the third peak was noisy and the least mean square logarithm could not reach a good fit and hence the data was fitted with two Gaussians, only.

## RESULTS

A total of 12 adult subjects participated in this study. Details of gender and appearance of the hair strands are listed in Table 1. About 10 strands were cut from the scalp, glued onto a

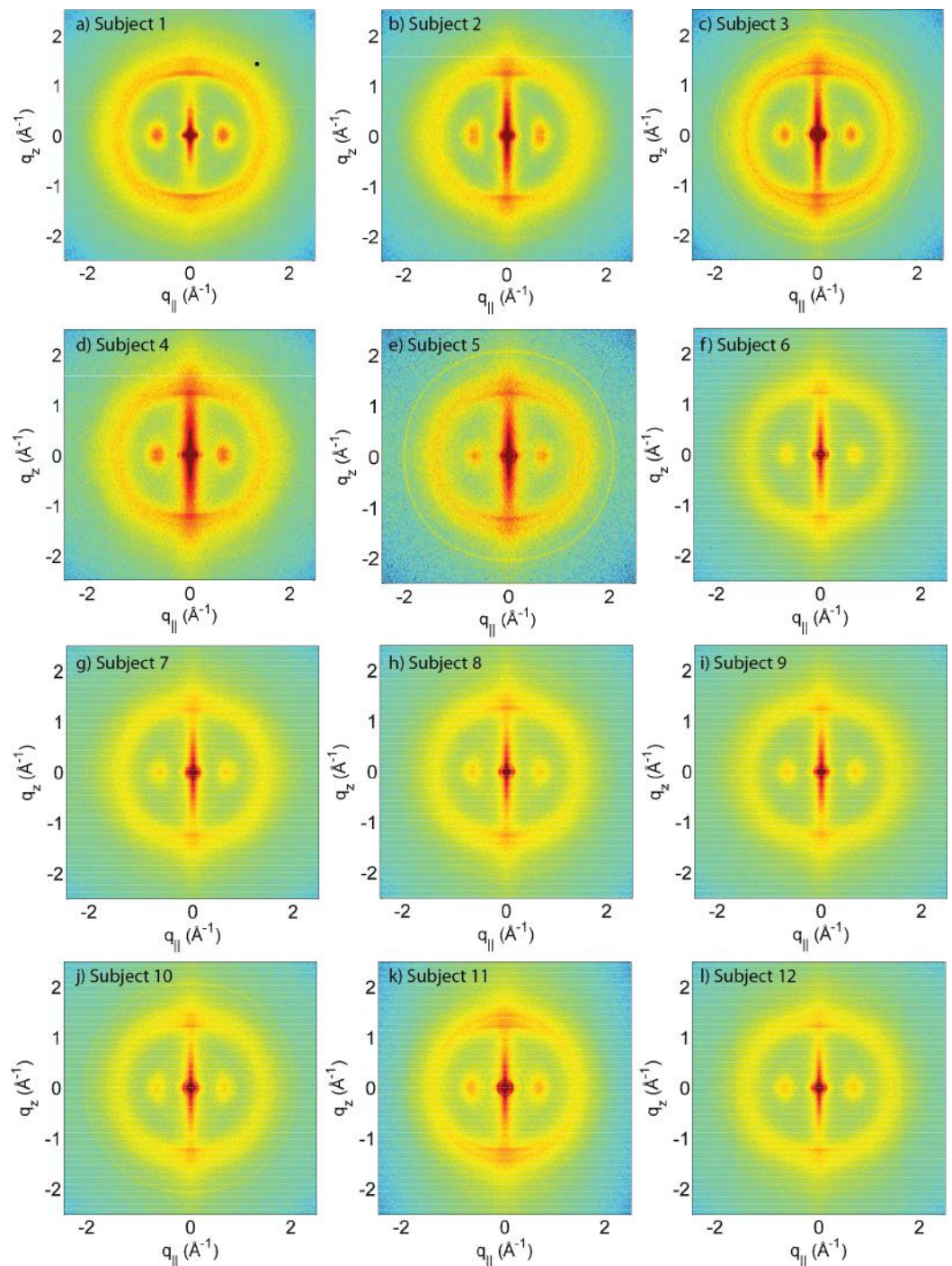


**Figure 1** Two-dimensional X-ray data of all 12 subjects. The hair strands were oriented with the long axis of the hair parallel to the vertical  $z$ -axis. The  $(q_{||}, q_z)$ -range shown was determined in preliminary experiments to cover the features observable by X-ray diffraction. The measurements cover length scales from about 3–90 Å to study features from the coiled-coil  $\alpha$ -keratin phase, keratin intermediate filaments in the *cortex*, and the membrane layer in the membrane complex. While common features can easily be identified in the 2D plots, subtle differences are visible, which are discussed in detail in the text.

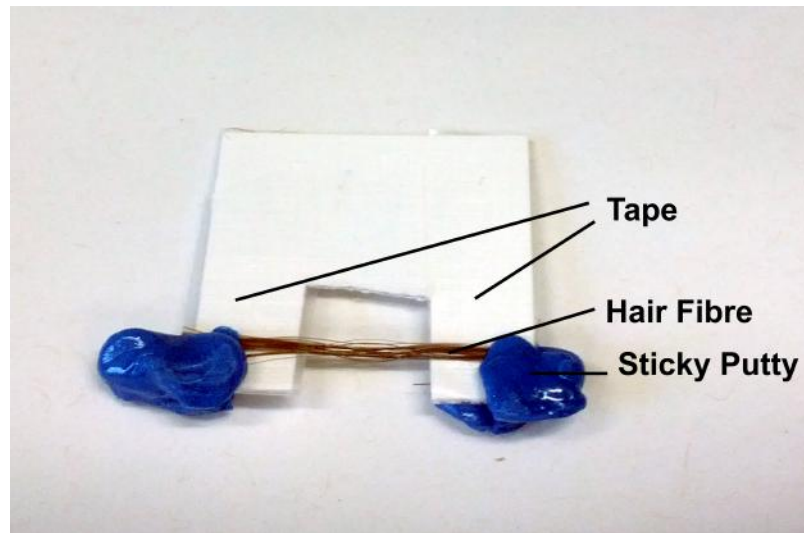


**Figure 2** The apparatus used to mount the hair strands in the experiment. The cardboard apparatus is mounted vertically onto the loading plate of the Biological Large Angle Diffraction Experiment (BLADE) using sticky putty.

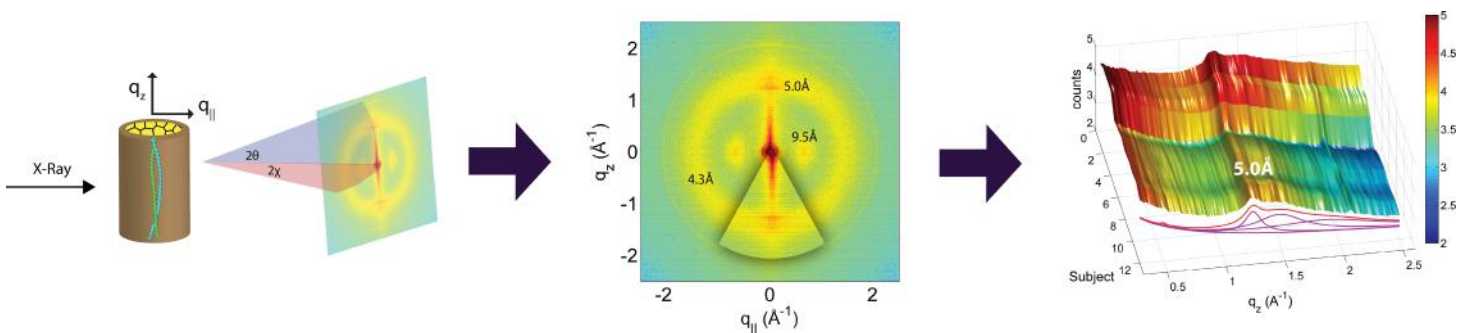


**Figure 3** Schematics of the X-ray setup and example X-ray data. The hair strands were oriented in the X-ray diffractometer with their long axis along  $q_z$ . Two-dimensional X-ray data were measured for each specimen covering distances from about 3–90 Å including signals from the coiled-coil  $\alpha$ -keratin phase, the intermediate fibrils in the *cortex* and from the cell membrane complex. The 2-dimensional data were integrated and converted into line scans and fit for a quantitative analysis.

sample holder and aligned in the X-ray diffractometer. The resulting 2-dimensional X-ray intensity maps of the reciprocal space reveal exquisite details of the molecular structure of human scalp hair, as presented in Fig. 1. The hair strands were oriented with the long axis of the hair parallel to the vertical  $z$ -axis. The displayed  $(q_z, q_{||})$ -range was determined to cover the length scales of the features of interest in preliminary experiments.

The data in Fig. 1 show a distinct non-isotropic distribution of the diffracted intensity with pronounced and well defined intensities along the long axis of the hair and in the equatorial plane (the  $q_z$  and  $q_{||}$ -axes, respectively), indicative of a high degree of molecular order in the hair strands. Some features were common in all specimens and assigned to certain molecular components, as explained in the next section.

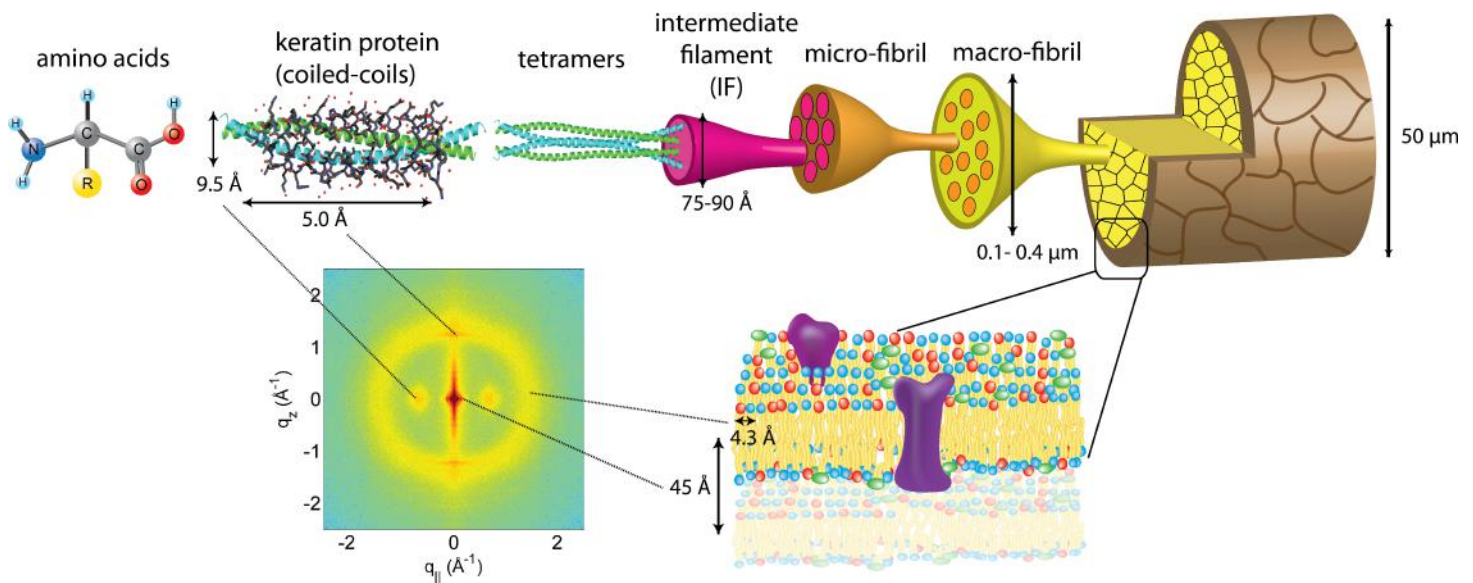


**Figure 4** The hierarchical structure of hair in the *cortex* and *cuticle*. The main component of the *cortex* is a keratin coiled-coil protein phase. The proteins form intermediate filaments, which then organize into larger and larger fibres. The hair is surrounded by the *cuticle*, a dead cell layer. The common features observed in the X-ray data of all specimens are signals related to the coiled-coil keratin phase and the formation of intermediate filaments in the *cortex*, and the cell membrane complex. Signal assignment and corresponding length scales are shown in the figure.

## Assignment of common scattering signals

### *Coiled-coil protein phase in the cortex*

The keratin proteins in the *cortex* are known to organize in bundles whose structures are dominated by  $\alpha$ -helical coiled-coils (Pauling & Corey, 1950; Pinto et al., 2014; Yang et al., 2014). The main features of this pattern are a  $\sim 9.5$  Å (corresponding to  $q_{\parallel} \sim 0.6$  Å<sup>-1</sup>) equatorial reflection corresponding to the spacing between adjacent coiled-coils and a  $\sim 5.0$  Å meridional reflection (corresponding to  $q_z \sim 1.25$  Å<sup>-1</sup>) corresponding to the superhelical structure of  $\alpha$ -helices twisting around each other within coiled-coils (Crick, 1952; Cohen & Parry, 1994; Lupas & Gruber, 2005). As displayed in Fig. 4, these signals were observed in the X-ray data in all specimen and assigned to the coiled-coil protein phase. We note that these peaks are related to generic  $\alpha$ -helical coil structures of monomeric proteins, and not specific to a certain type of protein.

### *Lipids in the cell membrane complex*

The cell membrane complex mainly consists of lipid mono- and bilayers. The corresponding scattering features correspond to a lamellar periodicity of about 45 Å, and rings at spacings of about 4.3 Å, characteristic of the order within the layers (Busson, Engstrom & Doucet, 1999). Both these features are observed in the 2-dimensional X-ray data of all individuals in Fig. 1, as a ring-like scattering intensity at  $q$ -values of  $\sim 0.1$  Å<sup>-1</sup> and a broad, ring-like scattering at  $\sim 1.5$  Å<sup>-1</sup> as a result of the lipid order within the membrane layers. The corresponding diffraction signal has a maximum on the  $q_z$ -axis, indicating a preferential orientation of the membrane plane parallel to the surface of the hair.

### **Intermediate filaments in the cortex**

The keratin coils organize into intermediate filaments whose structure and packing in the plane of the hair result in additional scattering signals. The packing of these fibrils by bundling into macro-fibrils is characterized by X-ray diffraction pattern by three equatorial spots located at about 90, 45 and 27 Å (Busson, Engstrom & Doucet, 1999). The corresponding signals are observed in the 2-dimensional data in Fig. 1. The exact position of the features is, however, best determined in small angle diffraction experiments (SAXS), which offer a drastically improved resolution, and will be shown below. We note that the axial packing of coiled-coils within keratin filaments in hair gives rise to a number of fine arcs along the meridian ( $z$ ). The typically observed signal on the meridian at 67 Å, which arises from the axial stagger between molecules along the microfibril (Briki et al., 2000; Rafik, Doucet & Briki, 2004), could not be observed in our experiments due to the relaxed resolution of the parallel beam in this direction. While the features observed in scattering experiments are well known, the molecular architecture of the intermediate filaments is still under discussion (Rafik, Doucet & Briki, 2004). Supercoiled coiled-coils or models that involve straight dimers with different numbers of coils are being discussed.

The three features above were observed in all individuals in Fig. 1. The underlying molecular structures will be quantitatively analyzed in the next section (Quantitative analysis of scattering results). We note that additional features are seen in some of the measurements in Fig. 1, mainly in the broad membrane ring at around  $1.5 \text{ \AA}^{-1}$  which indicates a difference in molecular composition of the cell membrane complex between individuals. We will come back to these differences in the Discussion.

### **Quantitative analysis of scattering results**

In order to quantitatively determine the position of the corresponding scattering features, the 2-dimensional data for all 12 individuals were integrated in the equatorial plane ( $q_{\parallel}$ -axis) of the hair fibres, and along the hair fibres ( $q_z$ -axis). The resulting plots are shown in Fig. 5. In the direction along the hair fibre axis ( $q_z$ ), there are two major peaks that were consistent among all subjects, one narrow peak around 5.0 Å and one broader peak around 4.3 Å.

In the direction perpendicular to the hair fibre axis ( $q_{\parallel}$ ), there are also two major peaks consistent among all subjects, one narrow peak around 9.5 Å and one broad peak around 4.3 Å. The total scattering profile was well fit by two Lorentzian peak profiles (and a background), whose positions is plotted in Fig. 5. The signals at 5.0 Å and 9.5 Å are in excellent agreement with signals reported from coiled-coil keratin proteins (Pauling & Corey, 1950), as depicted in the Figure. The broad signal at about 4.3 Å present in both directions is due to the ring-like scattering from the lipids in the membrane component. As plotted in Fig. 5, there is a narrow distribution of the corresponding length scales with standard deviations of  $9.51 \pm 0.07 \text{ \AA}$  and  $5.00 \pm 0.02 \text{ \AA}$  for the keratin coiled-coils and  $4.28 \pm 0.08 \text{ \AA}$  for the membrane signal, indicating that the common features observed in all individuals are well defined with little spread in the corresponding molecular dimensions.

Due to the large length scales involved, the signals from intermediate filaments occur at small scattering vectors, shown in Fig. 6. The Small Angle X-ray Scattering (SAXS)

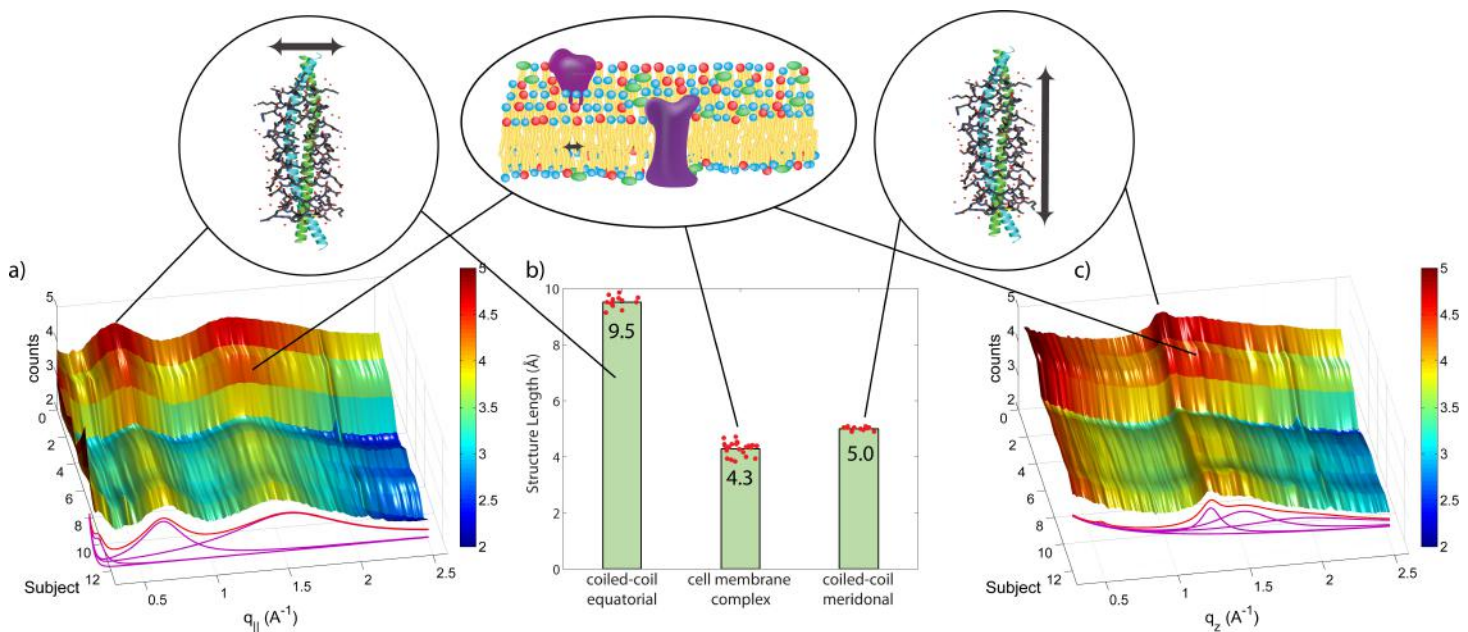


**Figure 5** Integration of the 2-dimensional scattering data in Fig. 1 in the equatorial plane ( $q_{\parallel}$ ) (A), and along the axis of the hairs ( $q_z$ ) (C), respectively, for all subjects. The two signals present in all individuals in the equatorial plane ( $q_{\parallel}$ ) correspond to the distance between two coiled coils of 9.5 Å and between two lipid tails in the cell membrane cortex of 4.3 Å. The common meridional signal along the long axis of the hair ( $q_z$ ) at 5 Å corresponds to the  $\alpha$ -helices twisting around each other within coiled-coils. Average values and standard deviations are in (B).

profile was well fit with three Gaussian peaks at 90 Å, 45 Å, and 27 Å. We note that the third peak was not observed in all hair samples. The corresponding peak positions and distributions are shown in the figure. The 90 Å peak has been reported early in the literature as the distance between intermediate filaments in human hair. As further elaborated by Rafik, Doucet & Briki (2004), these peaks correspond to the radial structures of the intermediate filaments and can be well-simulated by assuming parallel tetramers formed by 2 coiled-coils with a slight disorder in positions and orientations, as depicted in the figure. Also here, the standard deviations of  $90 \pm 2$  Å,  $47 \pm 2$  Å,  $27 \pm 1$  Å, as shown in the figure, are small, indicating that the organization of the intermediate filaments on the nanoscale varies very little between different individuals.

## DISCUSSION

All hair used in this study was in its native state, collected from healthy individuals and not chemically treated prior to the experiments. However, all individuals regularly used shampoos for cleaning and additional products such as conditioners, wax and gel. These products function primarily at or near the fiber surface to remove dirt from the hair surface, for instance, and do not seem to have an impact on the internal keratin structure, as will be discussed below.

An abnormal signal was previously reported by James *et al.* (1999) in hair samples of patients with breast cancer. Such an approach is quite intriguing, as scanning of hair samples could be used as easy, inexpensive and non-invasive screening techniques in the diagnosis of cancer. James *et al.* (1999) observed a ring-like signal at 44.4 Å, at the position

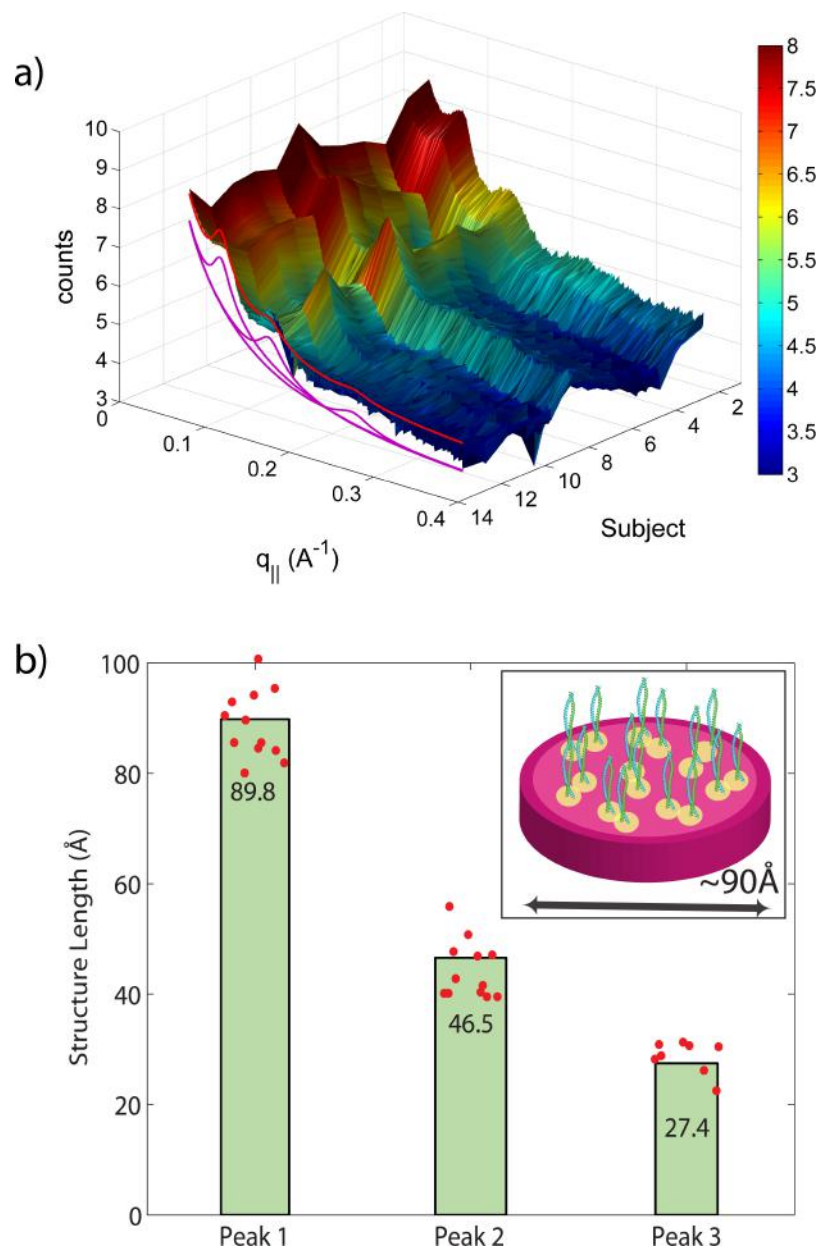


**Figure 6** Diffraction features at small scattering angles. The small  $q_{||}$ -range is shown in magnification in (A). The specimen of most individuals showed 3 distinct reflections at  $\sim 90$  Å, 46.5 Å and 27 Å, related to the properties of intermediate keratin filaments (B).

of the lamellar plasma membrane signal, and assigned this signal to the presence of breast cancer. The analysis and assignment was questioned later on by *Briki et al. (1999)* and *Howell et al. (2000)*, who observed this feature in healthy and cancer patients in equal measure. The ring-like 45 Å signal is also present in the data for all individuals included in our study, such that a relation to breast cancer can most likely be excluded.

## General structural features from the X-ray experiments

From the 2-dimensional X-ray data in Figs. 1 and 4, and the analysis in Figs. 5 and 6, we identify three features present in all individuals. These signals are related to the coiled-coils arrangement of the keratin proteins in the *cortex*, the formation of intermediate filaments in the *cortex*, and lipids in the cell membrane complex of the hair. Statistical analysis of the corresponding molecular dimensions revealed a rather small distribution between different individuals. These general properties of human hair are observed in all hair independent of gender, colour or optical appearance of the hair (as listed in Table 1) within the number of individuals included in this study.

Differences in the X-ray data between individuals were observed in the wide angle region (WAXS) of the 2-dimensional data in Fig. 1, related to properties of the membrane component. Figure 7A shows a comparison between individual 3 and 4 to illustrate the effect. For an easy comparison, the original data were cut in half and recombined, such that the left half depicts individual 3, and the right half individual 4. While signals from the coiled-coil protein phase, the diffuse, ring-like intensity from lipids in the cell membrane complex and the small angle signals due to the formation of intermediate filaments are observed in both individuals, additional signals occur in Subject 3 around the position of the membrane-ring. Almost identical patterns are observed in Figs. 7B and 7C, while differences are seen in Fig. 7D; this will be discussed in detail below.

The additional signals observed between about  $1.34 \text{ \AA}^{-1}$  and  $1.63 \text{ \AA}^{-1}$  can be assigned to fatty acids located within the plasma membrane of the cell membrane complex. The position of these lipids inside the hair was determined by synchrotron infrared microspectroscopy (Kreplak *et al.*, 2001a) detecting the corresponding  $\text{CH}_2$  and  $\text{CH}_3$  bands. The lipid component of the cell membrane complex consists of three major classes of lipids: glycerolipids (mainly phospholipids), sterols and sphingolipids (Furt, Simon-Plas & Mongrand, 2011). The most abundant lipid species are referred to as structural lipids up to 80% of which are phosphocholine (PC) and phosphoethanolamine (PE) phospholipids.

The position and width of the broad, ring-like intensity observed in all specimens in Fig. 1 agree well with lipid correlation peaks reported from single and multi-component phospholipid fluid lipid membranes (Kučerka *et al.*, 2005; Petrache *et al.*, 1998; Kuč, Tristram-Nagle & Nagle, 2006; Rheinstädter *et al.*, 2004; Rheinstädter, Seydel & Salditt, 2007; Rheinstädter *et al.*, 2008; Pan *et al.*, 2008; Schneggenburger *et al.*, 2011; Harroun *et al.*, 1999) and diffraction observed in plasma membranes (Welti *et al.*, 1981; Poinapen *et al.*, 2013). The broad correlation peak is the tell-tale sign of a fluid-like, disordered membrane structure. It is related to the packing of the lipid tails in the hydrophobic membrane core, where the lipid acyl chains form a densely packed structure with hexagonal symmetry (planar group  $p6$ ) (Armstrong *et al.*, 2013). The distance between two acyl tails is determined to be  $a_T = 4\pi/(\sqrt{3}q_T)$  (Mills *et al.*, 2008; Barrett *et al.*, 2012; Barrett *et al.*, 2013), where  $q_T$  is the position of the membrane correlation peak. The average nearest-neighbour distance between two lipid tails is calculated from the peak position to  $4.97 \text{ \AA}$ . We note that the intensity of the disordered membrane component is not distributed isotropically on a circle, which would be indicative of a non-oriented,

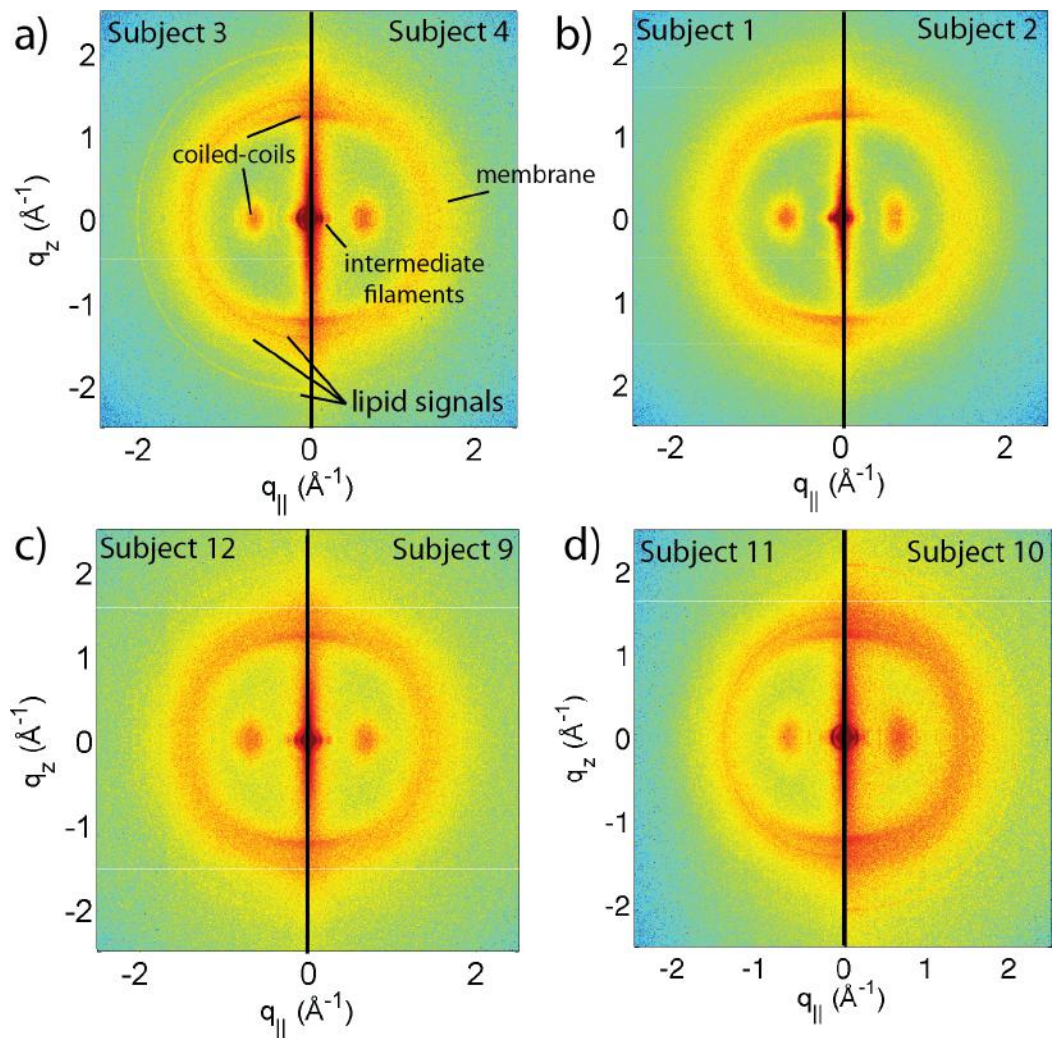


**Figure 7 Comparison between hair samples.** (A) shows a comparison between individuals 3 and 4. While the two specimens both show the general features, differences are observed in the region of signal from the cell membrane complex. (B) Comparison between individuals 1 and 2, father and daughter. The data in (C) (individuals 9 and 12) are from identical twins. Data in (D) was taken from fraternal twins (individuals 10 and 11). While different individuals in general show different membrane patterns (A), features in (B) and (C) perfectly agree. Fraternal twins show slight differences in their pattern in (D).

isotropic membrane phase. The corresponding scattering signal has a maximum along the  $q_z$ -axis, indicative that most of the membranes are aligned parallel to the hair surface.

The additional narrow components in Fig. 1 between about  $1.34 \text{ \AA}^{-1}$  and  $1.63 \text{ \AA}^{-1}$ , which are observed in some hair samples, agree with structural features reported in lipid membranes of different composition. A correlation peak at  $\sim 1.5 \text{ \AA}^{-1}$  was found in the gel phase of saturated phospholipid membranes, such as DMPC (Dimyristoyl-sn-glycero-3-phosphocholine) and DPPC (Dipalmitoyl-sn-glycero-3-phosphocholine) (Tristram-Nagle et al., 2002; Katsaras et al., 1995; Rheinstädter et al., 2004). Unsaturated lipids were reported to order in a structure with slightly larger nearest neighbour tail distances,

leading to an acyl-chain correlation peak at  $\sim 1.3 \text{ \AA}^{-1}$ , as reported for DOPC and POPC (Mills *et al.*, 2009), for instance. Lipids, such as Dimyristoylphosphatidylethanolamine (DMPE) and the charged DMPS (Dimyristoyl-sn-glycero-3-phosphoserine) with smaller head groups were reported to order in more densely packed structures (Rappolt & Rapp, 1996). The corresponding acyl chain correlation peaks were observed at Q values of  $\sim 1.65 \text{ \AA}^{-1}$ . The observed differences in the X-ray diffraction patterns between different individuals can, therefore, most likely be assigned to differences in the molecular composition of the plasma membrane in the cell membrane complex. Genetics plays an important role in this composition.

### Genetic similarity

Some subjects have genetic relations within the subject pool. In particular, Subject 1 and 2 are daughter and father, Subjects 10 and 11 are fraternal twins, and Subjects 9 and 12 are identical twins. The corresponding diffraction data are shown in Figs. 7B, 7C and 7D. While in general, the diffraction patterns in the membrane region were found to be different (as demonstrated in Fig. 7A), the genetically similar hair of father and daughter and identical twins show identical patterns within the resolution of our experiment.

It is interesting to note that differences are observed for the fraternal twins in Fig. 7D. This finding is in agreement with the expectation that individuals with similar genetics would share similar physical traits such as hair structure. Identical or monozygotic twins originate from one zygote during embryonic development, and they share 100% of their genetic material. Fraternal or dizygotic twins develop from the fertilization of two different eggs and they only share 50% of their DNA on average (Nussbaum *et al.*, 2007).

As expected, the identical twin pair shows almost identical hair structures whereas the fraternal pair exhibits distinct differences. Offspring receive half of their chromosomes from each parent, thus the genetic similarity between the parent and child pair is roughly the same as fraternal twins (Creasy *et al.*, 2013). It is, therefore, surprising that the father and daughter pair share significantly more similarities than the pair of fraternal twins. This can be attributed to the fact that the expression of a complex trait such as hair structure would depend on the inheritance pattern of many phenotype-determining genes, such as whether they are dominant or recessive traits. Genetic similarity does not guarantee identical hair structure and similarly, genetic variability does not guarantee differences. While we can report this finding, the small number of related samples excludes a more detailed and quantitative analysis of this effect at this time.

The comparison in Fig. 7B between father and daughter also enables the study of the effect of hair care products, such as shampoo and conditioner on the molecular structure of hair. While Subject 2 (father) uses soap and shower gel to clean scalp and hair, Subject 1 (daughter) regularly uses shampoo and conditioner. The identical X-ray signals indicate that these products do not have an effect on the molecular structure of keratin and membranes deep inside the hair (within the resolution of our experiment).

We note that in order to maximize the scattered signals, the entire hair strand was illuminated in our experiments using a relatively large X-ray beam. Microbeam X-ray

diffraction on synchrotron sources, which uses small, micrometre sized beams (*Iida & Noma, 1993; Busson, Engstrom & Doucet, 1999; Kreplak et al., 2001b; Ohta et al., 2005; Kajiura et al., 2006*), gives a high spatial resolution. By illuminating selective parts of the hair, the occurrence of the signals that we observed can be determined as a function of their location within the hair in future experiments.

## CONCLUSIONS

We studied the molecular hair structure of several individuals using X-ray diffraction. Hair samples were collected from 12 healthy individuals of various characteristics, such as gender, optical appearance and genetic relation. Signals corresponding to the coiled-coil phase of the keratin molecules, the formation of intermediate filaments in the *cortex* and from the lipid molecules in the cell membrane complex were observed in the experiment. The corresponding signals were observed in all individuals, independent of gender or appearance of the hair, such as colour or waviness, within the resolution of this experiment. Given the small standard deviation of the molecular dimensions of these general features, anomalies possibly related to certain diseases should be easy to detect.

While all hair samples showed these general features, differences between individuals were observed in the composition of the plasma membrane in the cell membrane complex. Genetics seem to play an important role in the properties of these membranes, as genetically similar hair samples from father and daughter and identical twins showed identical patterns, though hair from fraternal twins did not.

## ADDITIONAL INFORMATION AND DECLARATIONS

### Funding

This research was funded by the Natural Sciences and Engineering Research Council of Canada (NSERC), the National Research Council Canada (NRC), the Canada Foundation for Innovation (CFI) and the Ontario Ministry of Economic Development and Innovation. MCR is the recipient of an Early Researcher Award of the Province of Ontario. The funders had no role in study design, data collection and analysis, decision to publish, or preparation of the manuscript.

### Grant Disclosures

The following grant information was disclosed by the authors:  
Natural Sciences and Engineering Research Council of Canada (NSERC).  
National Research Council Canada (NRC).  
Canada Foundation for Innovation (CFI).  
Ontario Ministry of Economic Development and Innovation.

### Competing Interests

The authors declare there are no competing interests.

## Author Contributions

- Fei-Chi Yang, Yuchen Zhang and Maikel C. Rheinstädter conceived and designed the experiments, performed the experiments, analyzed the data, contributed reagents/materials/analysis tools, wrote the paper, prepared figures and/or tables, reviewed drafts of the paper.

## Human Ethics

The following information was supplied relating to ethical approvals (i.e., approving body and any reference numbers):

Hamilton Integrated Research Ethics Board (HIREB) under approval number 14-474-T.

## Supplemental Information

Supplemental information for this article can be found online at <http://dx.doi.org/10.7717/peerj.619#supplemental-information>.

## REFERENCES

- Armstrong CL, Marquardt D, Dies H, Kučerka N, Yamani Z, Harroun TA, Katsaras J, Shi A-C, Rheinstädter MC. 2013. The observation of highly ordered domains in membranes with cholesterol. *PLOS ONE* 8:e66162 DOI 10.1371/journal.pone.0066162.
- Astbury WT, Sisson WA. 1935. X-ray studies of the structure of hair, wool, and related fibres. III. The configuration of the keratin molecule and its orientation in the biological cell. *Proceedings of the Royal Society of London. Series A, Mathematical and Physical Sciences* 150:533–551 DOI 10.1098/rspa.1935.0121.
- Astbury WT, Street A. 1932. X-ray studies of the structure of hair, wool, and related fibres. I. General. *Philosophical Transactions of the Royal Society of London. Series A, Containing Papers of a Mathematical or Physical Character* 230:75–101 DOI 10.1098/rsta.1932.0003.
- Astbury WT, Woods HJ. 1934. X-ray studies of the structure of hair, wool, and related fibres. II. The molecular structure and elastic properties of hair keratin. *Philosophical Transactions of the Royal Society of London. Series A, Containing Papers of a Mathematical or Physical Character* 232:333–394 DOI 10.1098/rsta.1934.0010.
- Barrett MA, Zheng S, Roshankar G, Alsop RJ, Belanger RKR, Huynh C, Kučerka N, Rheinstädter MC. 2012. Interaction of aspirin (acetylsalicylic acid) with lipid membranes. *PLoS ONE* 7:e34357 DOI 10.1371/journal.pone.0034357.
- Barrett MA, Zheng S, Topozini LA, Alsop RJ, Dies H, Wang A, Jago N, Moore M, Rheinstädter MC. 2013. Solubility of cholesterol in lipid membranes and the formation of immiscible cholesterol plaques at high cholesterol concentrations. *Soft Matter* 9:9342–9351 DOI 10.1039/c3sm50700a.
- Berg BO, Rosenberg SH, Asbury AK. 1972. Giant axonal neuropathy. *Pediatrics* 49:894–899.
- Briki F, Busson B, Kreplak L, Dumas P, Doucet J. 2000. Exploring a biological tissue from atomic to macroscopic scale using synchrotron radiation: example of hair. *Cellular and Molecular Biology* 46:1005–1016.
- Briki F, Busson B, Salicru B, Estève F, Doucet J. 1999. Breast-cancer diagnosis using hair. *Nature* 400:226–226 DOI 10.1038/22244.

- Busson B, Engstrom P, Doucet J. 1999.** Existence of various structural zones in keratinous tissues revealed by X-ray microdiffraction. *Journal of Synchrotron Radiation* **6**:1021–1030 DOI [10.1107/S0909049599004537](https://doi.org/10.1107/S0909049599004537).
- Cohen C, Parry DA. 1994.** Alpha-helical coiled coils: more facts and better predictions. *Science* **263**:488–489 DOI [10.1126/science.8290957](https://doi.org/10.1126/science.8290957).
- Creasy RK, Resnik R, Iams JD, Lockwood CJ, Greene MF (eds.) 2013.** *Creasy and Resnik's maternal-fetal medicine: principles and practice*. WB Saunders.
- Crewther WG, Dowling LM, Steinert PM, Parry DAD. 1983.** Structure of intermediate filaments. *International Journal of Biological Macromolecules* **5**:267–274 DOI [10.1016/0141-8130\(83\)90040-5](https://doi.org/10.1016/0141-8130(83)90040-5).
- Crick FHC. 1952.** Is  $\alpha$ -keratin a coiled coil? *Nature* **170**:882–883 DOI [10.1038/170882b0](https://doi.org/10.1038/170882b0).
- Franbourg A, Hallegot P, Baltenneck F, Toutaina C, Leroy F. 2003.** Current research on ethnic hair. *Journal of the American Academy of Dermatology* **48**:S115–S119 DOI [10.1067/mjd.2003.277](https://doi.org/10.1067/mjd.2003.277).
- Fraser RD, MacRae TP, Parry DA, Suzuki E. 1986.** Intermediate filaments in alpha-keratins. *Proceedings of the National Academy of Sciences of the United States of America* **83**:1179–1183 DOI [10.1073/pnas.83.5.1179](https://doi.org/10.1073/pnas.83.5.1179).
- Fraser RD, MacRae TP, Rogers GE. 1962.** Molecular organization in alpha-keratin. *Nature* **193**:1052–1055 DOI [10.1038/1931052a0](https://doi.org/10.1038/1931052a0).
- Fraser RDB, MacRae TP, Sparrow LG, Parry DAD. 1988.** Disulphide bonding in  $\alpha$ -keratin. *International Journal of Biological Macromolecules* **10**:106–112 DOI [10.1016/0141-8130\(88\)90017-7](https://doi.org/10.1016/0141-8130(88)90017-7).
- Furt F, Simon-Plas F, Mongrand S. 2011.** Murphy AS, Schulz B, Peer W, eds. *The plant plasma membrane, Plant cell monographs*, vol. 19. Berlin, Heidelberg: Springer-Verlag, 57–85 DOI [10.1007/978-3-642-13431-9\\_1](https://doi.org/10.1007/978-3-642-13431-9_1).
- Harroun TA, Heller WT, Weiss TM, Yang L, Huang HW. 1999.** Experimental evidence for hydrophobic matching and membrane-mediated interactions in lipid bilayers containing gramicidin. *Biophysical Journal* **76**:937–945 DOI [10.1016/S0006-3495\(99\)77257-7](https://doi.org/10.1016/S0006-3495(99)77257-7).
- Howell A, Grossmann JG, Cheung KC, Kanbi L, D Gareth RE, Hasnain SS. 2000.** Can hair be used to screen for breast cancer? *Journal of Medical Genetics* **37**:297–298 DOI [10.1136/jmg.37.4.297](https://doi.org/10.1136/jmg.37.4.297).
- Iida A, Noma T. 1993.** Synchrotron X-ray muprobe and its application to human hair analysis. *Nuclear Instruments and Methods in Physics Research Section B: Beam Interactions with Materials and Atoms* **82**:129–138 DOI [10.1016/0168-583X\(93\)95092-J](https://doi.org/10.1016/0168-583X(93)95092-J).
- James V. 2001.** The importance of good images in using hair to screen for breast cancer. *Journal of Medical Genetics* **38**:e16 DOI [10.1136/jmg.38.5.e16](https://doi.org/10.1136/jmg.38.5.e16).
- James VJ, Amemiya Y. 1998.** Intermediate filament packing in  $\alpha$ -keratin of echidna quill. *Textile Research Journal* **68**:167–170 DOI [10.1177/004051759806800303](https://doi.org/10.1177/004051759806800303).
- James V, Kearsley J, Irving T, Amemiya Y, Cookson D. 1999.** Using hair to screen for breast cancer. *Nature* **398**:33–34 DOI [10.1038/17949](https://doi.org/10.1038/17949).
- Kajiura Y, Watanabe S, Itou T, Nakamura K, Iida A, Inoue K, Yagi N, Shinohara Y, Amemiya Y. 2006.** Structural analysis of human hair single fibres by scanning microbeam saxs. *Journal of Structural Biology* **155**:438–444 DOI [10.1016/j.jsb.2006.04.008](https://doi.org/10.1016/j.jsb.2006.04.008).
- Katsaras J, Raghunathan VA, Dufourcq EJ, Dufourcq J. 1995.** Evidence for a two-dimensional molecular lattice in subgel phase dppc bilayers. *Biochemistry* **34**:4684–4688 DOI [10.1021/bi00014a023](https://doi.org/10.1021/bi00014a023).

- Kreplak L, Briki F, Duvault Y, Doucet J, Merigoux C, Leroy F, Lévêque JL, Miller L, Carr GL, Williams GP, Dumas P. 2001a. Profiling lipids across Caucasian and Afro-American hair transverse cuts, using synchrotron infrared microspectrometry. *International Journal of Cosmetic Science* 23:369–374 DOI 10.1046/j.0412-5463.2001.00118.x.
- Kreplak L, Mérioux C, Briki F, Flot D, Doucet J. 2001b. Investigation of human hair cuticle structure by microdiffraction: direct observation of cell membrane complex swelling. *Biochimica et Biophysica Acta (BBA)—Protein Structure and Molecular Enzymology* 1547:268–274 DOI 10.1016/S0167-4838(01)00195-9.
- Kučerka N, Liu Y, Chu N, Petrache HI, Tristram-Nagle S, Nagle JF. 2005. Structure of fully hydrated fluid phase DMPC and DLPC lipid bilayers using X-ray scattering from oriented multilamellar arrays and from unilamellar vesicles. *Biophysical Journal* 88:2626–2637 DOI 10.1529/biophysj.104.056606.
- Kučerka N, Tristram-Nagle S, Nagle JF. 2006. Closer look at structure of fully hydrated fluid phase dppc bilayers. *Biophysical Journal* 90:L83–L85 DOI 10.1529/biophysj.106.086017.
- Lupas AN, Gruber M. 2005. The structure of  $\alpha$ -helical coiled coils. *Advances in Protein Chemistry* 70:37–38.
- Mercer EH. 1953. The heterogeneity of the keratin fibers. *Textile Research Journal* 23:388–397 DOI 10.1177/004051755302300603.
- Mills TT, Huang J, Feigenson GW, Nagle JF. 2009. Effects of cholesterol and unsaturated dppc lipid on chain packing of saturated gel-phase dppc bilayers. *General Physiology and Biophysics* 28:126–139 DOI 10.4149/gpb.2009.02.126.
- Mills TT, Toombes GES, Tristram-Nagle S, Smilgies D-M, Feigenson GW, Nagle JF. 2008. Order parameters and areas in fluid-phase oriented lipid membranes using wide angle X-ray scattering. *Biophysical Journal* 95:669–681 DOI 10.1529/biophysj.107.127845.
- Nussbaum RL, McInnes RR, Willard HF, Hamosh A. 2007. Principles of molecular disease: lessons from the hemoglobinopathies. In: *Thompson & Thompson genetics in medicine*, vol. 6, 181–202.
- Ohta N, Oka T, Inoue K, Yagi N, Kato S, Hatta I. 2005. Structural analysis of cell membrane complex of a hair fibre by micro-beam X-ray diffraction. *Journal of Applied Crystallography* 38:274–279 DOI 10.1107/S002188980403403X.
- Pan J, Mills TT, Tristram-Nagle S, Nagle JF. 2008. Cholesterol perturbs lipid bilayers nonuniversally. *Physical Review Letters* 100:198103 DOI 10.1103/PhysRevLett.100.198103.
- Pauling L, Corey RB. 1950. Two hydrogen-bonded spiral configurations of the polypeptide chain. *Journal of the American Chemical Society* 72:5349–5349 DOI 10.1021/ja01167a545.
- Pauling L, Corey RB. 1951. The structure of hair, muscle, and related proteins. *Proceedings of the National Academy of Sciences of the United States of America* 37:261–271 DOI 10.1073/pnas.37.5.261.
- Petrache HI, Gouliaev N, Tristram-Nagle S, Zhang R, Suter RM, Nagle JF. 1998. Interbilayer interactions from high-resolution X-ray scattering. *Physical Review E* 57:7014–7024 DOI 10.1103/PhysRevE.57.7014.
- Pinto N, Yang F-C, Negishi A, Rheinstädter MC, Gillis TE, Fudge DS. 2014. Self-assembly enhances the strength of fibers made from vimentin intermediate filament proteins. *Biomacromolecules* 15:574–581 DOI 10.1021/bm401600a.
- Poinapen D, Topozini L, Dies H, Brown DCW, Rheinstädter MC. 2013. Static magnetic fields enhance lipid order in native plant plasma membrane. *Soft Matter* 9:6804–6813 DOI 10.1039/c3sm50355k.

- Rafik M Er, Doucet J, Briki F. 2004.** The intermediate filament architecture as determined by X-ray diffraction modeling of hard  $\alpha$ -keratin. *Biophysical Journal* **86**:3893–3904 DOI [10.1529/biophysj.103.034694](https://doi.org/10.1529/biophysj.103.034694).
- Randebrook RJ. 1964.** Neue erkenntnisse über den morphologischen aufbau des menschlichen haares. *Journal of the Society of Cosmetic Chemists* **15**:691–706.
- Rappolt M, Rapp G. 1996.** Simultaneous small- and wide-angle X-ray diffraction during the main transition of dimyristoylphosphatidylethanolamine. *Berichte der Bunsengesellschaft and Physikalische Chemie* **7**:1153–1162 DOI [10.1002/bbpc.19961000710](https://doi.org/10.1002/bbpc.19961000710).
- Rheinstädter MC, Das J, Flenner EJ, Brüning B, Seydel T, Kosztin I. 2008.** Motional coherence in fluid phospholipid membranes. *Physical Review Letters* **101**:248106 DOI [10.1103/PhysRevLett.101.248106](https://doi.org/10.1103/PhysRevLett.101.248106).
- Rheinstädter MC, Ollinger C, Fragneto G, Demmel F, Salditt T. 2004.** Collective dynamics of lipid membranes studied by inelastic neutron scattering. *Physical Review Letters* **93**:108107 DOI [10.1103/PhysRevLett.93.108107](https://doi.org/10.1103/PhysRevLett.93.108107).
- Rheinstädter MC, Seydel T, Salditt T. 2007.** Nanosecond molecular relaxations in lipid bilayers studied by high energy resolution neutron scattering and in-situ diffraction. *Physical Review E* **75**:011907 DOI [10.1103/PhysRevE.75.011907](https://doi.org/10.1103/PhysRevE.75.011907).
- Robbins CR. 2012.** *Chemical and physical behavior of human hair*. 5th ed. New York: Springer.
- Rogers GE. 1959.** Electron microscopy of wool. *Journal of Ultrastructure Research* **2**:309–330 DOI [10.1016/S0022-5320\(59\)80004-6](https://doi.org/10.1016/S0022-5320(59)80004-6).
- Schneggenburger P, Beerlink A, Weinhausen B, Salditt T, Diederichsen U. 2011.** Peptide model helices in lipid membranes: insertion, positioning, and lipid response on aggregation studied by X-ray scattering. *European Biophysics Journal* **40**:417–436 DOI [10.1007/s00249-010-0645-4](https://doi.org/10.1007/s00249-010-0645-4).
- Swift JA, Smith JR. 2001.** Microscopical investigations on the epicuticle of mammalian keratin fibres. *Journal of Microscopy* **204**:203–211 DOI [10.1046/j.1365-2818.2001.00957.x](https://doi.org/10.1046/j.1365-2818.2001.00957.x).
- Tristram-Nagle S, Liu Y, Legleiter J, Nagle JF. 2002.** Structure of gel phase dmpc determined by X-ray diffraction. *Biophysical Journal* **83**:3324–3335 DOI [10.1016/S0006-3495\(02\)75333-2](https://doi.org/10.1016/S0006-3495(02)75333-2).
- Ward WH, Lundgren HP. 1954.** The formation, composition, and properties of the keratins. *Advances in Protein Chemistry* **9**:243–297.
- Welti R, Rintoul DA, Goodsaid-Zalduondo F, Felder S, Silbert DF. 1981.** Gel-phase phospholipid in the plasma membrane of sterol-depleted mouse lm cells. *The Journal of Biological Chemistry* **256**:7528–7535.
- Wilk KE, James VJ, Amemiya Y. 1995.** The intermediate filament structure of human hair. *Biochimica et Biophysica Acta (BBA)-General Subjects* **1245**:392–396 DOI [10.1016/0304-4165\(95\)00111-5](https://doi.org/10.1016/0304-4165(95)00111-5).
- Yang F-C, Peters RD, Dies H, Rheinstädter MC. 2014.** Hierarchical, self-similar structure in native squid pen. *Soft Matter* **10**:5541–5549 DOI [10.1039/C4SM00301B](https://doi.org/10.1039/C4SM00301B).